International Journal of Chemical, Materials and Biomolecular Sciences
ISSN: 2415-6620
Vol:10, No:5, 2016

# Influence of Raw Material Composition on Microstructure and Mechanical Properties of Nodular Cast Iron

Alan Vaško, Juraj Belan, Lenka Hurtalová, Eva Tillová

***Abstract*—**The aim of this study is to evaluate the influence of raw material composition on the microstructure, mechanical and fatigue properties and micromechanisms of failure of nodular cast iron. In order to evaluate the influence of charge composition, the structural analysis, mechanical and fatigue tests and microfractographic analysis were carried out on specimens of ten melts with different charge compositions. The basic charge of individual melts was formed by different ratio of pig iron and steel scrap and by different additive for regulation of chemical composition (silicon carbide or ferrosilicon). The results show differences in mechanical and fatigue properties, which are connected with the microstructure. SiC additive positively influences microstructure. Consequently, mechanical and fatigue properties of nodular cast iron are improved, especially in the melts with higher ratio of steel scrap in the charge.

***Keywords*—**Nodular cast iron, silicon carbide, microstructure, mechanical properties.

## I. Introduction

NODULAR cast iron is a group of cast structural materials with a wide application in engineering practice (especially in the automotive industry). It combines high tensile strength and plasticity with high fatigue strength. Nodular cast iron can be produced according to the classical or synthetic casting procedure (Fig. 1) which is more economical [1], [2].

From an economic point of view, the production of nodular cast iron has been orientated to synthetic melts in recent years. It means that a part of more expensive pig iron in a metal charge is substituted for cheaper steel scrap. The transition from the traditional use of pig iron (classical melts) to synthetic nodular cast iron prepared from steel scrap requires the regulation of chemical composition of melt. Steel scrap has low content of silicon; therefore, increasing of content of silicon to eutectic composition ($S_C \sim 1$) is reached by using of ferrosilicon (FeSi) or metallurgical silicon carbide (SiC) additive. Nowadays, there is the tendency to use metallurgical silicon carbide as a siliconizing agent as well as carburizing additive instead of ferrosilicon. SiC additive increases the count of crystallisation nuclei of graphite in the melt, consequently the count of graphitic nodules per unit of area is increased (the size of graphitic nodules is decreased) and at the same time the susceptibility to occurrence of carbide in the structure is decreased. Next influence of SiC additive is its ferritizing effect when the content of ferrite in the matrix is increased [3], [4].

The technological foundry literature describes the addition of SiC to the cast iron melt frequently as having a special pre-inoculating effect [5], [6]. This influence is well documented in the case of grey cast iron and has also been observed to some extent at laboratory as well as at industrial experiments in the case of nodular cast iron.

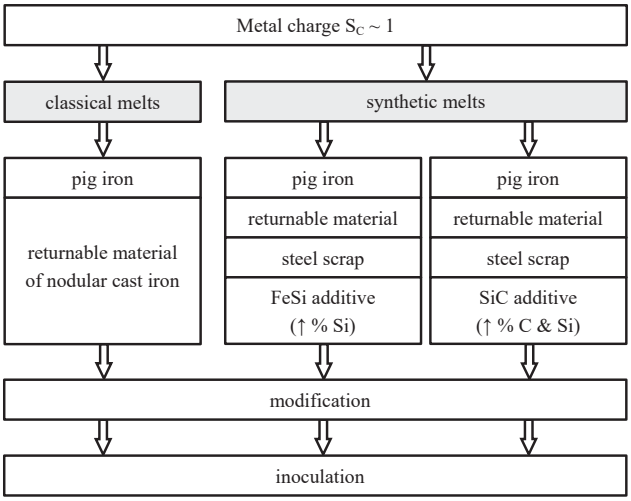


Fig. 1 Scheme of the production of nodular cast iron

The paper deals with the influence of charge composition on the microstructure, mechanical and fatigue properties and failure micro mechanisms of nodular cast irons. The basic charge of experimental melts was formed by a different ratio of pig iron and steel scrap. Chemical composition of individual melts was regulated alternatively by metallurgical silicon carbide or ferrosilicon and carburizer.

## II. Experimental Material and Methods

Two series of five melts of nodular cast iron were used for experiments. The resultant melts have approximately the same chemical composition but this was achieved by different charge composition (Table I). The basic charge of individual

A. Vaško is with the Department of Materials Engineering, Faculty of Mechanical Engineering, University of Žilina, Univerzitná 8215/1, 010 26 Žilina, Slovakia (corresponding author to provide phone: +421–41–5132605; fax: +421–41–5652940; e-mail: alan.vasko@fstroj.uniza.sk).

J. Belan, L. Hurtalová, and E. Tillová are with the Department of Materials Engineering, Faculty of Mechanical Engineering, University of Žilina, Univerzitná 8215/1, 010 26 Žilina, Slovakia (e-mail: juraj.belan@fstroj.uniza.sk, lenka.hurtalova@fstroj.uniza.sk, eva.tillova@fstroj.uniza.sk).

melts was formed by different ratio of pig iron and steel scrap and by different additive for the regulation of chemical composition. The ratio of steel scrap in the basic charge was increased gradually from 20 to 100% and the ratio of pig iron was decreased. For the regulation of chemical composition, the additive of carburizer and metallurgical silicon carbide was added to the melts 1 to 5 and the additive of carburizer and ferrosilicon was added to the melts 6 to 10. The content of these additives was chosen to achieve approximately the same resultant chemical composition of the melts (eutectic degree $S_c \approx 1.2$). For modification, FeSiMg7 modifier was used and for inoculation, FeSi75 inoculant was used.

Experimental bars (diameter 32 mm and length 350 mm) were cast from all melts. Experimental specimens for tensile test, impact bending test, hardness test and fatigue tests were made from experimental bars.

TABLE I
CHARGE COMPOSITION OF EXPERIMENTAL MELTS

| Melt number | Pig iron (%) | Steel scrap (%) | Additive | Modifier & inoculant |
|---|---|---|---|---|
| 1 | 80 | 20 | carburizer + SiC90 | FeSiMg7 FeSi75 |
| 2 | 60 | 40 | | |
| 3 | 40 | 60 | | |
| 4 | 20 | 80 | | |
| 5 | 0 | 100 | | |
| 6 | 80 | 20 | carburizer + FeSi75 | FeSiMg7 FeSi75 |
| 7 | 60 | 40 | | |
| 8 | 40 | 60 | | |
| 9 | 20 | 80 | | |
| 10 | 0 | 100 | | |

The metallographic analysis of specimens from experimental melts was made by the light metallographic microscope Neophot 32. The specimens for metallographic analysis were taken out from the cast bars and prepared by usual metallographic procedure. The microstructure of specimens was evaluated according to STN EN ISO 945 (STN 42 0461) and by automatic image analysis (using NIS Elements software) [7]. The image analysis was used for the evaluation of count of graphitic nodules per unit of area and content of ferrite in the matrix.

The tensile test was made according to STN EN ISO 6892-1 by means of the testing equipment ZDM 30 with a loading range F = 0 to 50 kN. The impact bending test was made according to STN EN ISO 148-1 by means of the Charpy hammer PSW 300 with a nominal energy of 300 J. The Brinell hardness test was made according to STN EN ISO 6506-1 by means of the testing equipment CV-3000 LDB with a hardmetal ball of diameter D = 10 mm forced into specimens under the load F = 29 430 N (3000 kp) [8].

The fatigue tests were made according to STN 42 0362 at high-frequency sinusoidal cyclic push-pull loading (frequency f ≈ 20 kHz, stress ratio R = –1, temperature T = 20 ± 5 °C) using the ultrasonic testing equipment KAUP-ZU [9]–[11].

The microfractographic analysis was made by the scanning electron microscopes Tesla BS 343 and VEGA II LMU on fracture surfaces of the specimens fractured by tensile test, impact bending test and fatigue tests [12].

## III. Experimental Results and Discussion

### A. Metallographic Analysis

From a microstructural point of view, the specimens from all the melts are ferritic-pearlitic nodular cast irons with different content of ferrite and pearlite in the matrix, different size of graphite and count of graphitic nodules (Fig. 2). Different content of ferrite and pearlite in the matrix as well as different size of graphite and count of graphitic nodules in the individual specimens are caused by different ratio of pig iron and steel scrap in the charge and by different kind of additive for the regulation of chemical composition (SiC or FeSi).

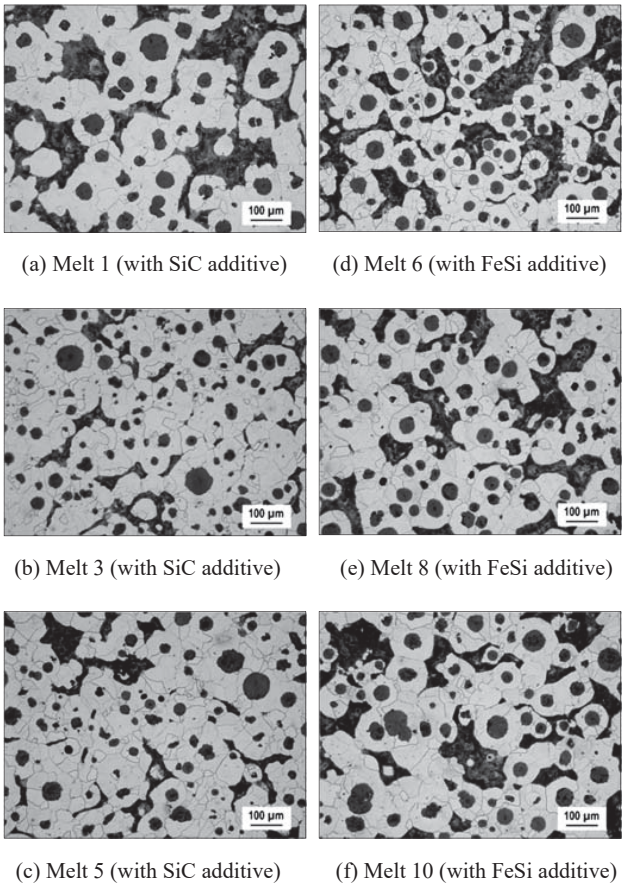


(a) Melt 1 (with SiC additive) (d) Melt 6 (with FeSi additive)

(b) Melt 3 (with SiC additive) (e) Melt 8 (with FeSi additive)

(c) Melt 5 (with SiC additive) (f) Melt 10 (with FeSi additive)

Fig. 2 Microstructure of the specimens from cast bars, etched 1% Nital

The results of the evaluation of the microstructure of the specimens from the cast bars by STN EN ISO 945 (STN 42 0461) and by image analysis (content of ferrite and count of graphitic nodules) are presented in Table II.

The content of ferrite in the specimens from the melts with SiC additive is higher than in the specimens from the melts with FeSi additive (Fig. 3 (a)). The highest content of ferrite was reached in the melt 5 created only by steel scrap and SiC additive (approximately 78%) and in the melt 3 created by

60% of steel scrap and SiC additive (74%).

TABLE II
EVALUATION OF THE MICROSTRUCTURE

| Melt number | Microstructure by STN EN ISO 945 | Content of ferrite (%) | Count of graphitic nodules ($mm^{-2}$) |
|---|---|---|---|
| 1 | 60%VI5/6 + 40%V6 – Fe80 | 61.6 | 104.3 |
| 2 | 80%VI5/6 + 20%V6 – Fe80 | 58.4 | 124.3 |
| 3 | 80%VI6 + 20%V6 – Fe94 | 74.0 | 199.8 |
| 4 | 80%VI5/6 + 20%V6 – Fe94 | 71.6 | 175.4 |
| 5 | 70%VI5/6 + 30%V6 – Fe94 | 78.0 | 179.8 |
| 6 | 70%VI5/6 + 30%V6 – Fe55 | 50.8 | 126.5 |
| 7 | 70%VI6 + 30%V6 – Fe80 | 62.8 | 131.0 |
| 8 | 70%VI5/6 + 30%V6 – Fe80 | 65.2 | 151.0 |
| 9 | 60%VI6 + 40%V6 – Fe80 | 58.8 | 133.2 |
| 10 | 70%VI5/6 + 30%V6 – Fe80 | 56.0 | 157.6 |

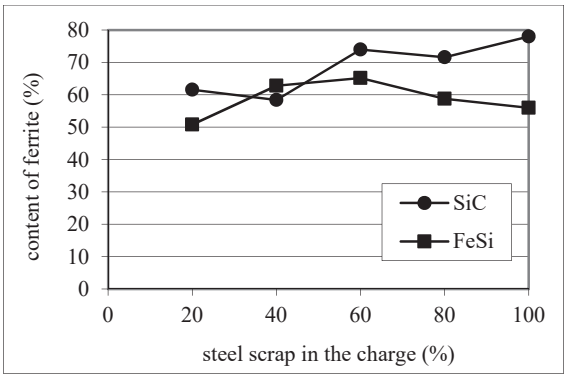


(a) Content of ferrite in the matrix

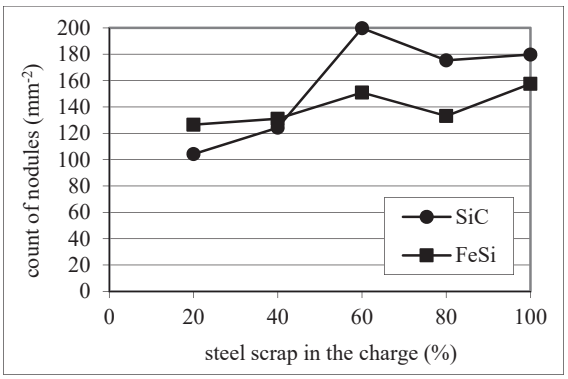


(b) Count of graphitic nodules

Fig. 3 Evaluation of the microstructure by image analysis

Graphite occurs only in a perfectly-nodular and imperfectly-nodular shape in all of the specimens. The ratio of perfectly-nodular graphite in the specimens from the melts with SiC additive is higher than in the specimens from the melts with FeSi additive. The size of graphite is from 30 to 120 μm, but in all the specimens the size within 30-60 μm predominates. The size of graphite in the specimens from the melts with SiC additive is generally smaller than in the specimens from the melts with FeSi additive. The average count of graphitic nodules per unit area in the specimens from the melts with SiC additive is higher than in the specimens from the melts with FeSi additive (Fig. 3 (b)). The highest count of graphitic nodules is in the melt 3 created by 60% of steel scrap and SiC additive (almost 200 $mm^{-2}$) and in the melt 5 created only by steel scrap and SiC additive (180 $mm^{-2}$).

### *B. Mechanical Properties*

The mechanical tests (i.e. tensile test, impact bending test and Brinell hardness test) were realized on the specimens made from the cast bars. The results of mechanical tests, i.e. tensile strength $R_m$, elongation A, absorbed energy K and Brinell hardness HB, are given in Table III.

TABLE III
MECHANICAL PROPERTIES

| Melt number | $R_m$ (MPa) | A (%) | K (J) | HBW 10/3000 |
|---|---|---|---|---|
| 1 | 500.8 | 1.3 | 6.4 | 210.0 |
| 2 | 432.9 | 3.0 | 19.4 | 181.7 |
| 3 | 539.0 | 4.0 | 30.6 | 192.3 |
| 4 | 527.4 | 3.8 | 23.9 | 187.3 |
| 5 | 515.7 | 3.7 | 17.2 | 182.3 |
| 6 | 367.1 | 1.7 | 8.4 | 190.0 |
| 7 | 515.6 | 3.7 | 27.8 | 175.7 |
| 8 | 462.6 | 2.7 | 24.0 | 181.3 |
| 9 | 488.1 | 3.3 | 24.8 | 176.3 |
| 10 | 462.6 | 2.7 | 19.2 | 183.0 |

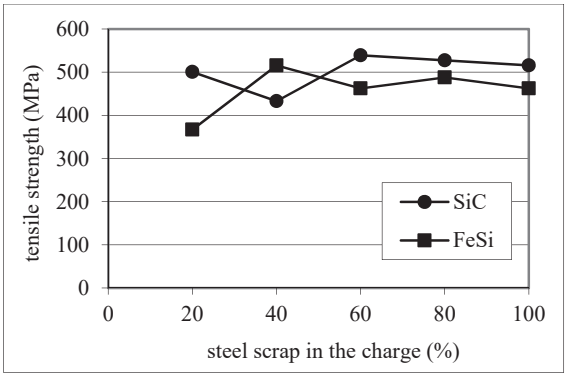


(a) Tensile strength

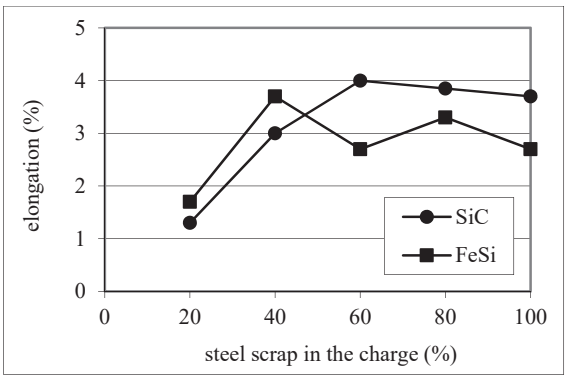


(b) Elongation

Fig. 4 Mechanical properties of the specimens

The tensile strength in the specimens from the melts with SiC additive is higher than in the specimens from the melts with FeSi additive (Fig. 4 (a)). The highest tensile strength (539 MPa) was reached in the melt 3 created by 60% of steel scrap and SiC additive. The elongation and absorbed energy in the specimens from the melts with SiC additive are also higher than in the specimens from the melts with FeSi additive (Fig. 4 (b)). The highest elongation (approximately 4%) as well as absorbed energy (above 30 J) were again reached in the melt 3 created by 60% of steel scrap and SiC additive.

The specimens from the melts with SiC additive have better mechanical properties than the specimens from the melts with FeSi additive. It has connection with the microstructure of the specimens, especially with the character of matrix (content of ferrite and pearlite) and also with the size and count of graphitic nodules. The best mechanical properties were reached in the melt 3 created by 60% of steel scrap and SiC additive, which has the highest ratio of perfectly-nodular graphite, the smallest size of graphite and the highest count of graphitic nodules.

*C. Fatigue Properties*

For the fatigue tests, ten specimens from each melt were used to obtain Wöhler fatigue curves $\sigma_a = f(N)$ and determine fatigue strength $\sigma_c$ for $N = 10^8$ cycles. The specimens were loaded by high-frequency sinusoidal cyclic push-pull loading (loading frequency $f \approx 20$ kHz).

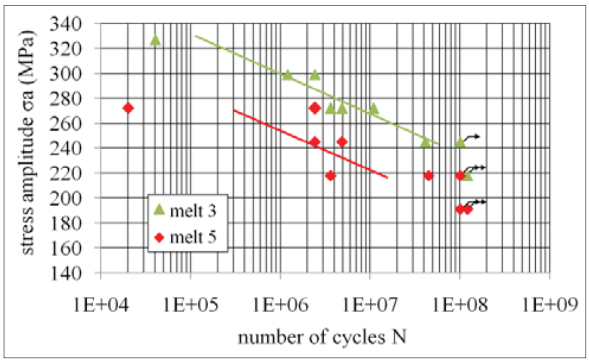


(a) Melts 3 and 5 (with SiC additive)

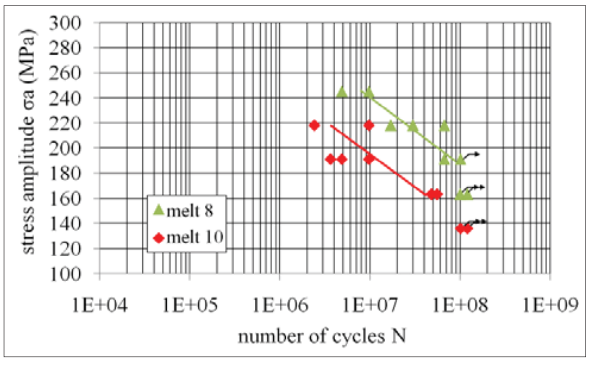


(b) Melts 8 and 10 (with FeSi additive)

Fig. 5 Wöhler curves $\sigma_a = f(N)$

The results of fatigue tests (relationship between stress amplitude $\sigma_a$ and number of cycles to failure $N_f$) are shown in Fig. 5. Obtained data were approximated by the Basquin function [9] with using of least square method. The number of cycles to failure increases with a decreasing stress amplitude.

The fatigue strength in analysed specimens of nodular cast iron increases with an increasing tensile strength. The fatigue strength in the specimens from the melts with SiC additive is higher than in the specimens from the melts with FeSi additive. The highest fatigue strength (218 MPa) was reached in the melt 3 created by 60% of steel scrap and SiC additive, which has also the best mechanical properties.

*D. Microfractographic Analysis*

The microfractographic analysis was made by the scanning electron microscope Tesla BS 343 on fracture surfaces of specimens from experimental bars fractured by the static tensile test (Fig. 6) and the impact bending test (Fig. 7).

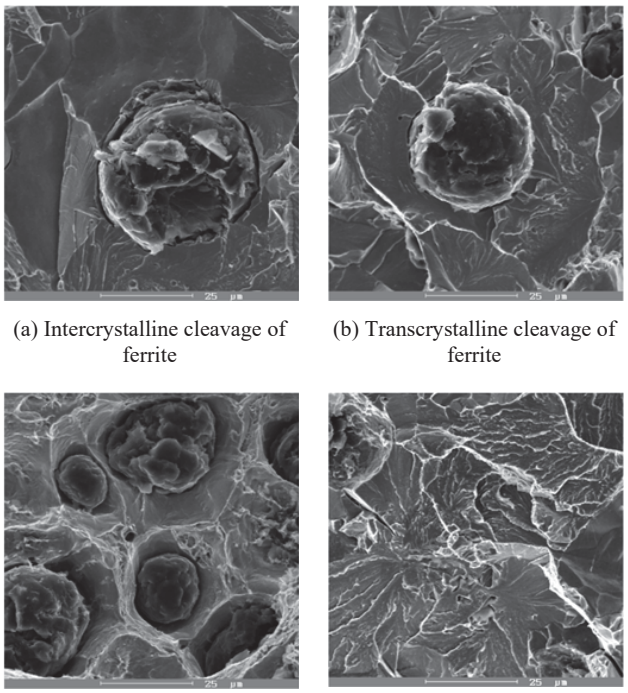

(a) Intercrystalline cleavage of ferrite

(b) Transcrystalline cleavage of ferrite

(c) Transcrystalline ductile failure of ferrite

(d) Transcrystalline continuous cleavage of pearlite

Fig. 6 Failure micro mechanisms at static stress, SEM

Fracture surfaces of the specimens fractured by the static tensile test are characteristic of mixed mode of fracture. In the specimens from the melts with lower content of ferrite in the matrix, transcrystalline cleavage of ferrite with an inclination to intercrystalline cleavage of ferrite around graphitic nodules (Fig. 6 (a)) was observed. In the specimens from the melts with higher content of ferrite in the matrix, transcrystalline cleavage of ferrite with river drawing on facets (Fig. 6 (b)) and transcrystalline ductile failure of ferrite with dimple morphology (Fig. 6 (c)) was observed. The ratio of transcrystalline ductile failure of ferrite (at the expense of

transcrystalline cleavage) is increased with increasing content of ferrite in the matrix. Pearlite was failured especially by transcrystalline continuous cleavage (Fig. 6 (d)) in all the specimens. In the specimens with higher content of ferrite in the matrix, also transcrystalline ductile failure of pearlite was observed. Similarly, fracture surfaces of the specimens fractured by the impact bending test are characteristic of mixed mode of fracture. In the specimens from the melts with lower content of ferrite in the matrix, intercrystalline cleavage of ferrite was observed around graphitic nodules (Fig. 7 (a)) and transcrystalline cleavage of ferrite in the rest of area. In the specimens from the melts with higher content of ferrite in the matrix, transcrystalline cleavage of ferrite with river drawing on facets (Fig. 7 (b)) and transcrystalline ductile failure of ferrite with dimple morphology (Fig. 7 (c)) was observed. The ratio of transcrystalline ductile failure of ferrite (at the expense of transcrystalline cleavage) is increased with increasing content of ferrite in the matrix. In all the specimens, transcrystalline continuous cleavage of pearlite (Fig. 7 (d)) as well as transcrystalline ductile failure of pearlite was observed.

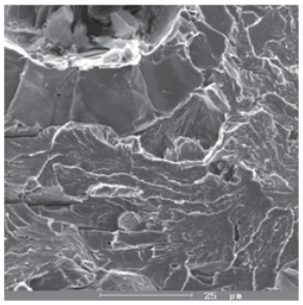

(a) Intercrystalline cleavage of ferrite

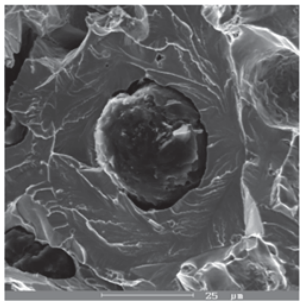

(b) Transcrystalline cleavage of ferrite

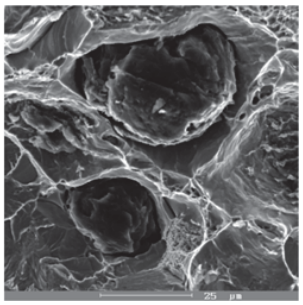

(c) Transcrystalline ductile failure of ferrite

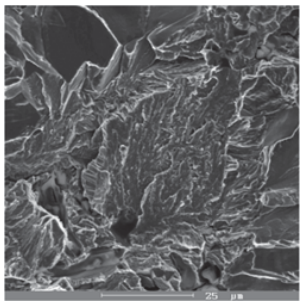

(d) Transcrystalline continuous cleavage of pearlite

Fig. 7 Failure micromechanisms at impact stress, SEM

The results of microfractographic analysis correspond to the results of metallographic analysis and mechanical tests. The microfractographic analysis of the specimens from experimental bars fractured by fatigue tests was made by the scanning electron microscope VEGA II LMU (Fig. 8). The fracture surfaces of analysed specimens do not show any remarkable differences; they are characteristic of mixed mode of fracture.

The fatigue fracture of the specimen from the melt 3 (with SiC additive) was initiated by casting defect (Fig. 8 (a)). The fatigue fracture is characteristic of intercrystalline fatigue failure of ferrite around graphitic nodules and transcrystalline fatigue failure of ferrite and pearlite in the rest of the area (Fig. 8 (b)). The final rupture is characteristic of transcrystalline ductile failure of ferrite with dimple morphology (Fig. 8 (c)) and transcrystalline cleavage of ferrite and pearlite with river drawing on facets (Fig. 8 (d)).

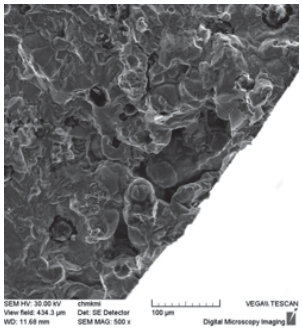

(a) Initiation of fatigue failure

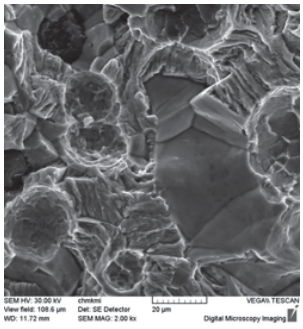

(b) Trans- and intercrystalline fatigue failure

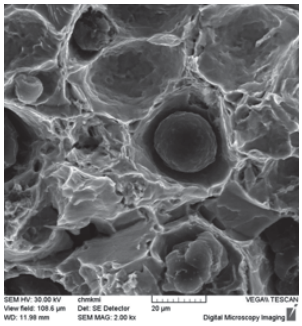

(c) Final rupture – transcrystalline ductile failure

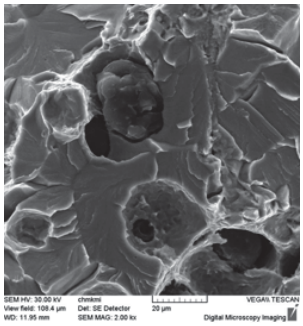

(d) Final rupture – transcrystalline cleavage

Fig. 8 Failure micromechanisms at fatigue stress, SEM (specimen from the melt 3, $\sigma_a$ = 272 MPa, $N_f$ = 1,1 x $10^7$ cycles)

No significant difference was observed by the comparison of fracture surfaces of the specimens from the analysed melts. The fatigue failure has a mixed character of fracture (intercrystalline and transcrystalline fatigue failure) in all the specimens; the intercrystalline fatigue failure predominates near graphitic nodules and the transcrystalline fatigue failure predominates in the rest of the area.

## IV. Conclusion

The results of the experiments show that the raw material composition influences the microstructure, mechanical as well as fatigue properties of nodular cast iron. The substitution of a part of pig iron for steel scrap in the charge of nodular cast iron has a considerable economic contribution. For the regulation of chemical composition of the melt it is advantageous to use the metallurgical SiC additive which has

been used in this work as an alternative additive instead of FeSi in melts with a different ratio of steel scrap in the charge. The experimental results can be summarized to the points:

- The SiC additive positively influences the microstructure, it means the content of ferrite in the matrix is increased, the size of graphite is decreased and the average count of graphitic nodules per unit of area is increased; consequently, the mechanical and fatigue properties of nodular cast iron are improved;
- The best mechanical and fatigue properties from the analysed specimens were reached in the specimens from the melt 3 created by 60% of steel scrap and 40% of pig iron in the basic charge with SiC additive;
- Micromechanisms of failure of structural components depends especially on the content of ferrite in the matrix and its purity, which has a connection with the charge composition; higher ratio of transcrystalline ductile failure is characteristic for higher content of ferrite in the matrix.

## ACKNOWLEDGMENT

This work has been supported by the Scientific Grant Agency of Ministry of Education, Science, Research and Sport of Slovak Republic, grant project No. 1/0533/15 and project of European Union ITMS 26110230117.

## REFERENCES

[1] R. Konečná, V. Konstantová, and G. Nicoletto, "Sizing of defects and fatigue behavior of nitrided nodular cast irons," *Materials Science (Medžiagotyra)*, vol. 14, pp. 215-220, 2008.
[2] P. Skočovský, and T. Podrábský, *Graphitic cast irons*. Žilina: EDIS, 2005.
[3] T. Benecke, S. Venkateswaran, W.D. Schubert, and B. Lux, "Investigation of the influence of silicon carbide in the production of ductile cast iron," *Foundryman*, vol. 87, pp. 355-360, October 1994.
[4] R. Gerhardt, *Properties and applications of silicon carbide*. Rijeka: InTech, 2011.
[5] K.W. Copi, Y.S. Lerner, and N.S. Laukhin, "SiC vs. 75% FeSi: Comparing pre-inoculation effects," *Modern Casting*, vol. 93, pp. 29-31, April 2003.
[6] W.H. Zhang, J. Ding, and F.R. Nie, "SiC inoculation pretreatment of cast iron," *Zhuzao/Foundry*, vol. 58, pp. 279-281, March 2009.
[7] P. Skočovský, and A. Vaško, *Quantitative evaluation of structure of cast irons*. Žilina: EDIS, 2007.
[8] A. Vaško, and P. Skočovský, *Properties and using of metal materials*. Žilina: EDIS, 2014.
[9] O. Bokůvka, G. Nicoletto, M. Guagliano, L. Kunz, P. Palček, F. Nový, *Fatigue of materials at low and high frequency loading*. Žilina: EDIS, 2014.
[10] M. Sága, P. Kopas, and M. Uhríčik, "Modeling and experimental analysis of the aluminium alloy fatigue damage in the case of bending-torsion loading," *Procedia Engineering*, vol. 48, pp. 599-606, 2012.
[11] M. Vaško, and M. Sága, "Application of fuzzy structural analysis for damage prediction considering uncertain S/N curve," *Applied Mechanics and Materials*, vol. 420, pp. 21-29, 2013.
[12] R. Konečná, and B. Hadzimová, "Microfractography of nodular cast iron," *Transactions of Famena*, vol. 26, pp. 59-65, 2002.